

X-ray Microbeam Strain Measurements in Polycrystalline Films

G. S. Cargill III,¹ L. Moyer,¹ Wenge Yang,² B. C. Larson,² and G. E. Ice²

¹ Dept. Mat. Sci. and Engr., Lehigh Univ., Bethlehem, PA 18018, USA,
gsc3@lehigh.edu, ler2@lehigh.edu

² Solid State Div., Oak Ridge National Lab., Oak Ridge, TN 37831 USA,
yangw@ornl.gov, bcl@ornl.gov, gei@ornl.gov

Keywords: x-ray, microbeam, residual strain, electromigration

Abstract

Two approaches to x-ray microbeam diffraction measurements in polycrystalline films are described: white beam measurements with an energy dispersive detector, which are suitable when grain sizes are much smaller than the x-ray beam size, and white and scanned energy x-ray diffraction measurements with a CCD detector, which are suitable when grain sizes are larger than or on the same order as the x-ray beam size. The former approach gives spatially resolved strain measurements which average over many grains, and the latter approach provides maps of grain orientations and triaxial strains on a grain by grain basis. Examples are shown for polycrystalline Al and Cu films.

Introduction

X-ray diffraction is a well established method for measuring elastic strains in polycrystalline materials on centimeter and millimeter length scales [1], but new techniques are being developed to obtain spatially resolved strain measurements at micron and submicron levels. Conventional methods for x-ray diffraction strain measurements require that the sample being studied be rotated with respect to the incident x-ray beam in order to obtain diffraction from differently oriented sets of planes needed to determine different components of the strain. However, unintended translations of samples during these rotations, because of limited mechanical precision and off-axis parallax, seriously limit the spatial resolution which can be obtained by this approach. Improvements in spatial resolution have been made by using x-ray diffraction methods which do not require sample rotations and by using high brightness synchrotron x-ray sources and pinholes, tapered glass capillaries, or Kirkpatrick-Baez focusing mirrors to form micron or submicron diameter x-ray beams.

A white beam energy dispersive microdiffraction technique, described in Fig. 1, is useful when the polycrystalline grain size is much smaller than the desired spatial resolution, which determines the size of the incident x-ray beam which must be used [2-4]. Rotating the energy dispersive solid state detector (SSD) with respect to the sample and the incident x-ray beam permits diffraction to be measured for scattering vectors \mathbf{k} making different angles with respect to the sample's plane normal \mathbf{n} , as required to obtain different components of the elastic strain. From the detector angles α and β , the scattering angle 2θ can be calculated, and from the SSD output, the energy, and wavelength λ , of the diffracted x-rays can be obtained. From 2θ and λ , Bragg's law is used to calculate the interplanar spacing d_{hkl} . The elastic strain in the direction of the scattering vector \mathbf{k} is obtained from d_{hkl} and the strain-free spacing d_{hkl}^0 for the material being studied.

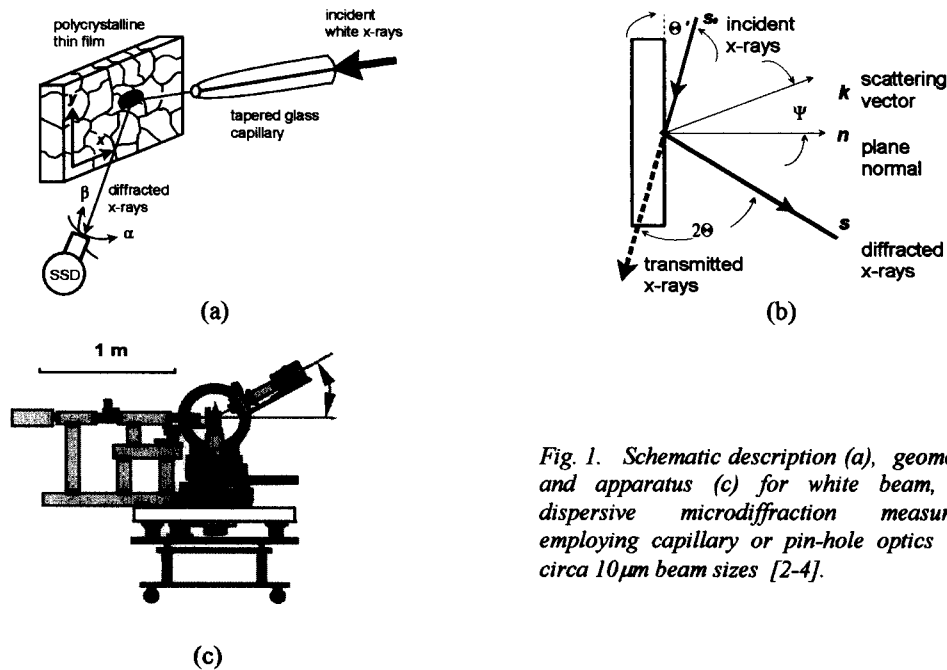


Fig. 1. Schematic description (a), geometry (b), and apparatus (c) for white beam, energy dispersive microdiffraction measurements, employing capillary or pin-hole optics to form circa $10\mu\text{m}$ beam sizes [2-4].

Another white beam microdiffraction technique is described in Fig. 2. This method uses an area x-ray detector, based on a charge coupled device (CCD) with a phosphor screen and optical fiber coupler, to record Laue diffraction patterns from individual grains which are illuminated by the incident x-ray microbeam [5,6]. This method is useful when the polycrystalline grain size is larger than or on the same order as the incident x-ray beam size, so that only one, or a small number, of grains contribute to each Laue pattern. Computer programs have been developed to index the Laue patterns, even when several differently oriented grains contribute to a pattern. These data are used to obtain grain orientation and strain tensor maps of polycrystalline films [7].

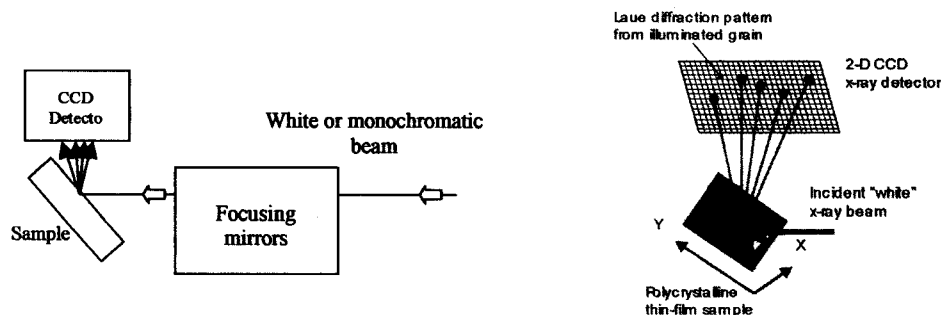


Fig. 2. Schematics of a white and scanned energy microbeam technique [5,6], using Kirkpatrick-Baez focusing mirrors to form a circa $0.5\mu\text{m}$ beam size and a CCD detector to record the Laue diffraction patterns, with a moveable, scanning monochromator (not shown) for absolute strain measurements, or a white beam for deviatoric strain measurements.

Even without determining the x-ray wavelengths responsible for the different Laue reflections, the angles between the diffracted beams can be analyzed to yield the components ε_{ij}^* of the deviatoric strain tensor for each diffracting grain [7],

$$\varepsilon_{ij}^* = \begin{pmatrix} \varepsilon_{11}^* & \varepsilon_{12}^* & \varepsilon_{13}^* \\ \varepsilon_{12}^* & \varepsilon_{22}^* & \varepsilon_{23}^* \\ \varepsilon_{13}^* & \varepsilon_{23}^* & \varepsilon_{33}^* \end{pmatrix} = \begin{pmatrix} \varepsilon_{11} - \frac{\Delta}{3} & \varepsilon_{12} & \varepsilon_{13} \\ \varepsilon_{12} & \varepsilon_{22} - \frac{\Delta}{3} & \varepsilon_{23} \\ \varepsilon_{13} & \varepsilon_{23} & \varepsilon_{33} - \frac{\Delta}{3} \end{pmatrix} \quad (1)$$

where $\Delta = \varepsilon_{11} + \varepsilon_{22} + \varepsilon_{33}$. To determine the absolute strains ε_{ij} for a grain, at least one interplanar spacing d_{hkl} must be determined, and the strain free value d_{hkl}^0 must be known. This is accomplished by inserting a scanning monochromator into the incident x-ray beam and using it to determine the x-ray energy, and wavelength λ , for one of the Laue reflections. The scattering angle 2θ is determined from the position of the reflection on the CCD, and Bragg's law is used to determine d_{hkl} from λ and 2θ . Larson et al. [8] have also developed methods to obtain three-dimensional mapping of grain orientations and strains by an extension of this technique.

Strain Measurements Using Energy Dispersive White Beam X-ray Microdiffraction

Particularly useful applications of energy dispersive white beam microdiffraction with a $10\mu\text{m}$ beam size have been in real time studies of electromigration-induced strains in $10\mu\text{m}$ wide, $0.5\mu\text{m}$ thick passivated Al and Al(Cu) conductor line samples, as shown in Fig. 3. Changes in (111) interplanar spacings were measured for grains with (111) planes parallel to the film plane. The samples had a strong (111) fiber texture and $0.5\mu\text{m}$ grain size, so several grains within the $10\mu\text{m}$ diameter irradiated area contributed to the (111) diffraction. Results $a_{\text{eff}} = \sqrt{3}d_{111}$ obtained at room temperature and at two elevated temperatures are shown in Fig. 4(a) for different locations along a $200\mu\text{m}$ long conductor line, and average values at each temperature are shown in Fig. 4(b) to agree well with those expected for a laterally confined film with equi-biaxial thermal stress [3].

Electromigration-induced strains measured with this technique are shown in Fig. 5(a) for a pure Al conductor line, and in Fig. 5(b) for an Al(0.25 at.% Cu) conductor line. The linear strain gradient along the full length of the pure Al conductor line results from a balance between electromigration and stress gradient forces [9]. The strain gradient extends along only part of the length of the Al(Cu) conductor line, because Cu concentrations were high enough to prevent Al electromigration in the $130\mu\text{m}$ - $200\mu\text{m}$ part of the line [10]. In the experiments on Al(Cu), x-ray microbeam fluorescence was used to monitor Cu concentration distributions.

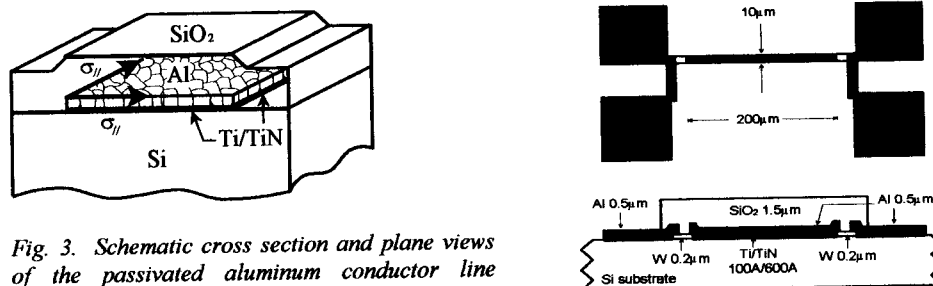


Fig. 3. Schematic cross section and plane views of the passivated aluminum conductor line sample, from [3].

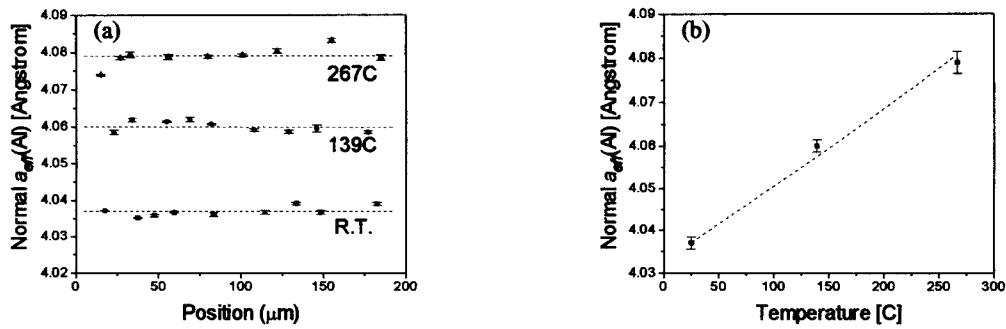


Fig. 4. (a) The measured a_{eff} values for positions along the passivated $10\mu\text{m}$ -wide Al line at different temperatures. (b) The averaged a_{eff} values versus temperature (data points) and the calculated a_{eff} for a laterally confined film with equi-biaxial stress (dashed line). From [3].

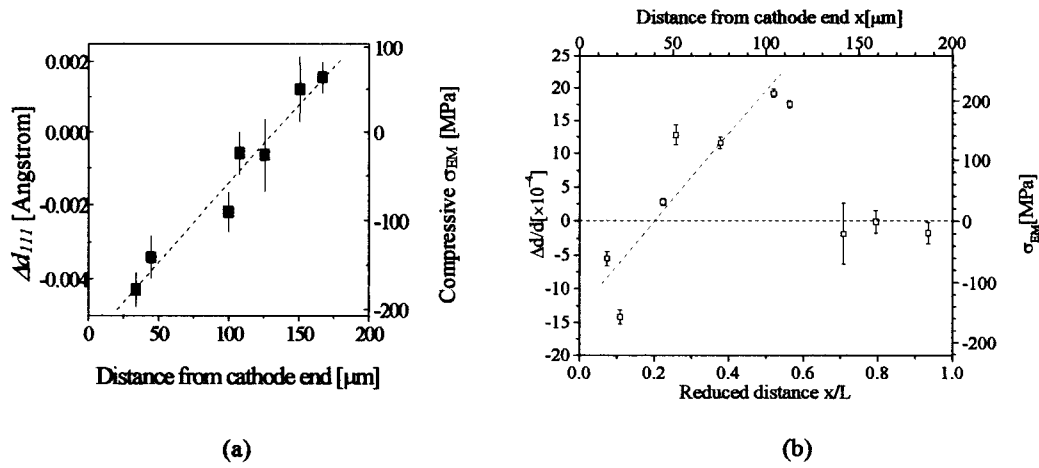


Fig. 5. (a) Electromigration-induced Al (111) plane spacing changes Δd_{111} and corresponding compressive stresses σ_{EM} measured at several positions along an aluminum conductor line after nine hours of electromigration. A linear stress gradient of $1.8\text{ MPa}/\mu\text{m}$ was induced by electromigration, as shown by the linear fit dashed line, from [9]. (b) Strains determined from electromigration-induced Al(111) plane spacing changes and corresponding compressive stresses at different positions along the Al(Cu) conductor line after 42 hrs of electromigration, from [10].

Grain Orientation and Strain Mapping Using a CCD Detector and White or Scanned Energy X-ray Microdiffraction

Several studies of grain orientation and strain mapping using a CCD detector and white or scanned energy x-ray microdiffraction have been published by groups at the Advanced Photon Source [5] and at the Advanced Light Source [6]. This technique was used in a recent study of residual strains in a polycrystalline $1\mu\text{m}$ thick Cu film on a $200\mu\text{m}$ thick oxidized Si substrate, with a 150\AA thick Cr barrier layer between the Cu film and the substrate [11]. The sample was heated to 400°C , held for one hour, and cooled to room temperature immediately before the x-ray measurements. It had a (111) fiber texture and an average grain size of approximately $1\mu\text{m}$, but with some much larger grains.

Figure 6 shows grain orientations from a 5 x 15 array of 75 different CCD images of Laue patterns for a 2.5 μm x 7.5 μm region of the film. Most of the patterns had significant contributions from one, two, or three different grains. The grain orientation map in Fig. 6 shows a large area of (111) grain orientations. Locations of grain boundaries within individual 0.5 μm x 0.5 μm squares, each corresponding to a single CCD image, are drawn to indicate which grains contribute, but the location of the boundaries within the squares have not been specifically determined.

Deviatoric strains ϵ_{33}^* perpendicular to the film plane and ϵ_{11}^* and ϵ_{22}^* within the film plane were determined for each (111) Laue pattern for the area shown in Fig. 6. The distributions of these strain values are shown in Fig. 7. The average value of $\epsilon_{33}^* = -0.0022$ is negative, as expected for residual thermal strain at room temperature after annealing the Cu-on-Si sample at elevated temperature. The average values of the two in-plane strain components are nearly equal, or equibiaxial, as expected for thermal strains in a blanket film. These data also show that there is significant variation in residual strain even among grains with the same crystallographic orientation.

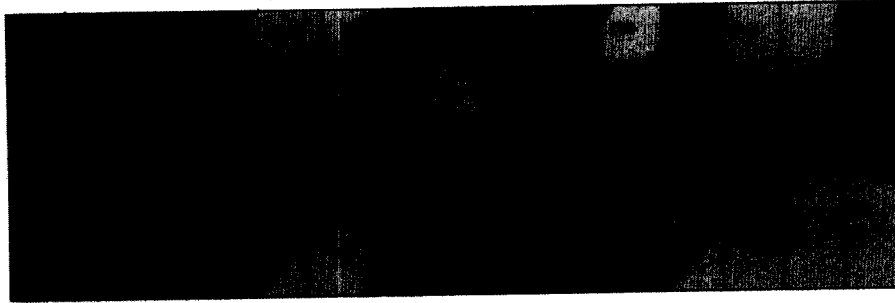


Fig. 6. Grain orientation map of 2.5 μm x 7.5 μm area of Cu thin film sample.

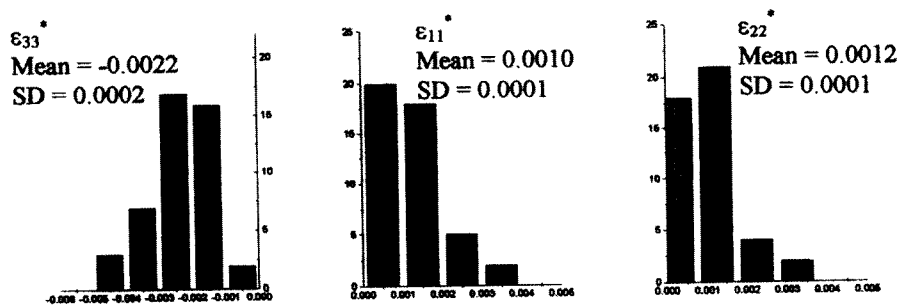


Fig. 7. Distributions of deviatoric strains for all (111) grains shown in Fig. 6.

Figure 8 repeats the left third of the grain orientation map from Fig. 6, and it shows the distribution of ϵ_{33}^* values for nine 0.5 μm x 0.5 μm square areas of the large (111) oriented grain, in which ϵ_{33}^* ranges between -1.6 to -3.1×10^{-3} , as shown in the 3 x 3 color coded map. It is interesting to note the large strain variation within the overall 1.5 μm x 1.5 μm area, that the lowest strain values are clustered along the left side, adjacent to the (110) oriented grain, and that the three squares with highest strains are adjacent to one another. The absolute strain ϵ_{33} was determined by energy scanning for the central (111) oriented grain, indicated by the white border in Fig. 8. The value obtained, $\epsilon_{33} = -1.1 \times 10^{-3}$, together with the deviatoric strain $\epsilon_{33}^* = -1.7 \times 10^{-3}$, gives a value of $\Delta = 3(\epsilon_{33} - \epsilon_{33}^*) = 1.8 \times 10^{-3}$. Further analysis is needed to characterize fully residual strains in this sample.

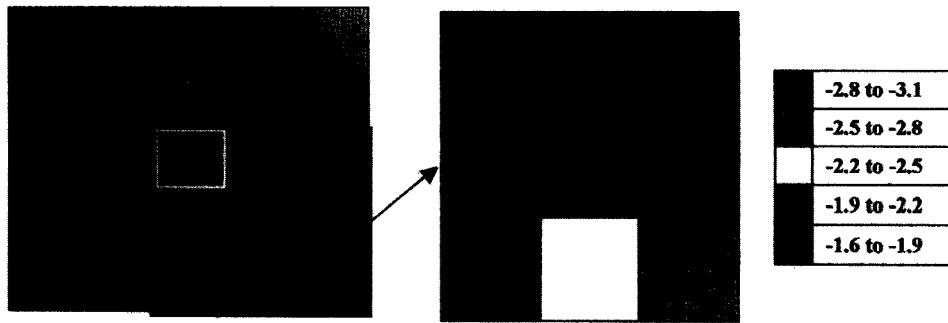


Fig. 8. Deviatoric strain variations within a single (111) grain. Strain values are $\times 10^{-3}$.

Conclusions

Recent developments permit measurements of strain in polycrystalline films with micron and submicron spatial resolution. Choices between white beam energy dispersive microdiffraction and area detection, white and scanned energy microdiffraction depend upon whether the grain size is much smaller than the x-ray beam size, or is on the same order or larger than the x-ray beam size. In the former case, white beam energy dispersive microdiffraction provides grain-averaged strains, and in the latter case, area detection, white and scanned energy microdiffraction provided intra- and inter-granular strain values.

Acknowledgements: This research was supported in part by NSF grants DMR-9796284 and DMR-9896002 at Columbia University and Lehigh University and by the SURA/ORNL Summer Cooperative Research Program, and it was carried out in part at the National Synchrotron Light Source, Brookhaven National Laboratory, which is supported by the U.S. Department of Energy, Division of Materials Sciences and Division of Chemical Sciences, under Contract No. DE-AC02-98CH10886. ORNL research was sponsored by the US Department of Energy, Basic Energy Sciences, Division of Materials Sciences under contract DE-AC05-00OR22725 with Oak Ridge National Laboratory, managed by UT-Battelle, LL. Work performed on the UNICAT beamline at the APS was supported in part by DoE Grant No. DE-FG02-99ER45743; UNI-CAT is operated by UIUC, ORNL, NIST, and UOP Research, Inc. The operation of the APS is sponsored by the DoE.

References

1. C. Noyan and J. B. Cohen, *Residual Stress* (Springer-Verlag, New York, 1987).
2. P.-C. Wang, G. S. Cargill III, and I. C. Noyan, *MRS Symp. Proc.* **375**, 247 (1995).
3. P.-C. Wang, G. S. Cargill III, I. C. Noyan, E. G. Liniger, C.-K. Hu, and K. Y. Lee, *MRS Symp. Proc.* **427**, 35 (1996).
4. G. S. Cargill III, A. C. Ho, K. J. Hwang, H. K. Kao, P.-C. Wang, and C.-K. Hu, *MRS Symp. Proc.* **563**, 157 (1999).
5. J.-S. Chung, N. Tamura, G. E. Ice, B. C. Larson, and J. D. Budai, *MRS Symp. Proc.* **563**, 169 (1999).
6. N. Tamura et al., *Appl. Phys. Letters* **80**, 3724 (2002).
7. J.-S. Chung and G. E. Ice, *J. Appl. Phys.* **86**, 5249 (1999).
8. B. C. Larson, W. Yang, G. E. Ice, J. D. Budai, and J. Z. Tischler, *Nature* **415**, 887 (2002).
9. P.-C. Wang, G. S. Cargill III, I. C. Noyan, and C.-K. Hu, *Appl. Phys. Letters* **72**, 1296 (1998).
10. H.-K. Kao, G. S. Cargill III, F. Giuliani, and C.-K. Hu, *J. Appl. Phys.*, to appear, March, 2003.
11. L. Moyer, G. S. Cargill III, B. C. Larson, and W. Wang, unpublished.